Angular Momentum and Cross Sections for Fusion with Weakly Bound Nuclei: Breakup, a Coherent Effect

Vandana Tripathi, A. Navin,* K. Mahata, K. Ramachandran, A. Chatterjee, and S. Kailas

Nuclear Physics Division, Bhabha Atomic Research Centre, Mumbai 400085, India

(Received 25 October 2001; published 11 April 2002)

Results for the cross section and average angular momentum for complete fusion at energies around the Coulomb barrier are presented for ^{7}Li with ^{165}Ho. Comparison of the cross sections with a one-dimensional barrier penetration model, using a potential consistent with the measured elastic scattering, showed a reduction above the barrier and an enhancement below it. An increase in the measured average angular momentum, $\langle \ell \rangle$, above the barrier and its consistency with that obtained from the fusion excitation function for weakly bound nuclei, is reported. These results together with a reanalysis of existing data conclusively demonstrate that the effect of breakup on fusion is *coherent*, like coupling to any nonelastic channel.

DOI: 10.1103/PhysRevLett.88.172701 PACS numbers: 25.70.Jj, 25.60.Gc, 25.60.Pj, 25.70.Mn

The understanding of the fusion process using radioactive ion beams (RIB) has great ramifications both for the production of superheavy elements (SHE) and in reactions of astrophysical interest. The weak binding of the valence nucleon(s) in RIB results in an extended spatial extent (halo/skin) and a large breakup cross section, both strongly influencing the fusion of these nuclei [1]. Fusion of heavy ions is treated as a tunneling phenomenon depending on the intrinsic degrees of freedom in addition to the radial separation of the colliding nuclei [2]. The role of inelastic excitations and few nucleon transfer has been illustrated from precise measurements of the fusion excitation function covering a wide range of $Z_p Z_t$ [3]. However, the influence of the projectile breakup on fusion is not yet well understood [4].

Two theoretical models having different perspectives have been proposed to understand the effect of projectile breakup on fusion. The first [5,6] treats breakup as causing an attenuation of the flux (E and ℓ dependent) in the incident channel. The transmission coefficients for fusion are thus multiplied by a breakup survival probability leading to smaller fusion cross sections and reduced values of $\langle \ell \rangle$. This implies that the two channels, the elastic and the broken-up products, can fuse *incoherently* leading to complete and breakup fusion, respectively. In contrast to this intuitive approach, the role of breakup can be considered in a coupled channel formalism like an inelastic excitation to the continuum [7]. This would mean that the fusing system is a *coherent* superposition of the elastic and breakup channels and will always lead to an enhancement of the complete fusion cross section below the Coulomb barrier and a suppression above it, compared to a one-dimensional barrier penetration model (1D-BPM) prediction [8]. The main difference between the two approaches viz. the coherent or incoherent role of breakup on fusion has to be resolved experimentally. Analyses of experiments with weakly bound stable (^{9}Be) [9] and radioactive beams of ^{6}He [10,11] and ^{11}Be [4] have not resolved the issue. One of the reasons is the ambiguity in the choice of the reference potential used in the calculations.

The measurement of the angular momentum of the fused system will give an additional handle to address this problem. It has been pointed out earlier [12–14] that under simple assumptions the two observables, angular momentum and fusion cross sections, are not independent and a relationship between the moments of ℓ and the fusion excitation function exists which is model independent. The main assumption here is that the transmission coefficient $T_\ell(E)$ follow the relationship $T_\ell(E) = T_0(E')$, where $E' = E - \beta(E)\ell(\ell + 1)$ and $\beta(E)$ can be thought about as the inverse of a generalized moment of inertia. As pointed out by Balantekin [13] the above does not necessarily imply that the fusion process is governed by an effective one-dimensional, energy-independent local potential barrier. The transmission coefficients in the approach treating breakup as an incoherent loss of flux [5,6] do not satisfy the relationship mentioned above, because of the energy dependence of the breakup survival probability factor, while the coupled channel approach does. Hence, the measurement of $\langle \ell \rangle$ and its consistency with that derived from the fusion excitation function will be an independent test of the validity of the two models.

With the aim of experimentally addressing the coherent or incoherent effect of the breakup channel on the fusion process at energies around the Coulomb barrier (V_b) , we report results on complete and breakup fusion cross section and average angular momentum using a weakly bound ^{7}Li projectile (breakup threshold of 2.45 MeV for the $\alpha + t$ channel) on the ^{165}Ho target. A consistent analysis of the present work along with relevant work in the literature, within a coupled channel framework, is presented to illustrate the coherent role of projectile breakup on fusion.

Measurements were performed using a ^{7}Li beam, from the 14UD BARC-TIFR Pelletron Accelerator Facility at Mumbai, in the energy range 23 to 45 MeV corresponding to $0.9V_b$ to $1.7V_b$. The 3.8 mg/cm^2 thick ^{165}Ho target was backed by 800 μg/cm^2 thick Bi (measured using

Rutherford scattering). The cross sections for complete fusion (CF) leading to the compound nuclei ^{172}Yb were obtained from the sum of the $2n$–$5n$ evaporation residue (ER) cross sections. The intensities of the low lying characteristic γ rays, emitted from the deformed ER, were measured using an efficiency calibrated Compton suppressed HpGe detector to obtain the corresponding cross sections. For the even-even ER (^{168,170}Yb) the cross sections were extracted from the extrapolated value of the intensity at $J = 0$ obtained from the measured γ-ray intensities for various transitions in the ground state rotational band. For the $3n$ channel (^{169}Yb) the cross sections were obtained using the measured intensity of the $5/2^-$ state at 191.2 keV and the measured ratios of the cross sections for $3n(^{168}\text{Yb})/4n(^{167}\text{Yb})$ in the ^{6}Li + ^{165}Ho system at three energies, corresponding to the same excitation energy as in the ^{7}Li case and using the statistical model code CASCADE [15,16]. The cross section for the $5n$ channel (^{167}Yb) was obtained by following its radioactive decay to ^{167}Tm with a $t_{1/2}$ of 17.5 min. The cross section for CF as a function of the center of mass energy is shown in Fig. 1. Cross sections for the dominant channel ($2n$) in the decay of ^{168}Er formed in breakup fusion (t + ^{165}Ho) are also shown in Fig. 1. The cross sections for the other decay channels are expected to be small except at the highest energies [17] and could not be obtained. The corresponding α + ^{165}Ho fusion cross sections are much smaller due to the higher Coulomb barrier and can be correlated to the large α yield in the exit channel [18]. The errors in the cross section include uncertainties in the target thickness, efficiency of the detector, and the integrated beam current.

In order to explore the consistency of the nuclear potential used in the calculations and the importance of various direct reaction channels, angular distributions were measured at an energy of 41.7 MeV ($E \gg V_b$), using two ΔE-E telescopes for elastic and important direct reactions, and are shown in Fig. 2. The solid curve in Fig. 2 corresponds to an optical model calculation using the code ECIS [19] with the *same* real part of the nuclear potential [Akyüz Winther (AW) parametrization [20]) as used in the calculations shown in Figs. 1 and 3. The volume imaginary part used was chosen to reproduce the measured reaction cross section at this energy. As seen from Fig. 2 the AW potential is a good choice and can be used as a reference 1D potential for further calculations. A potential that fits the complete fusion cross section at energies above the barrier is inconsistent with the measured elastic scattering angular distribution (dashed line in Fig. 2). The large cross sections (395 mb) for the breakup (could include a small contribution from transfer) and the small cross sections for

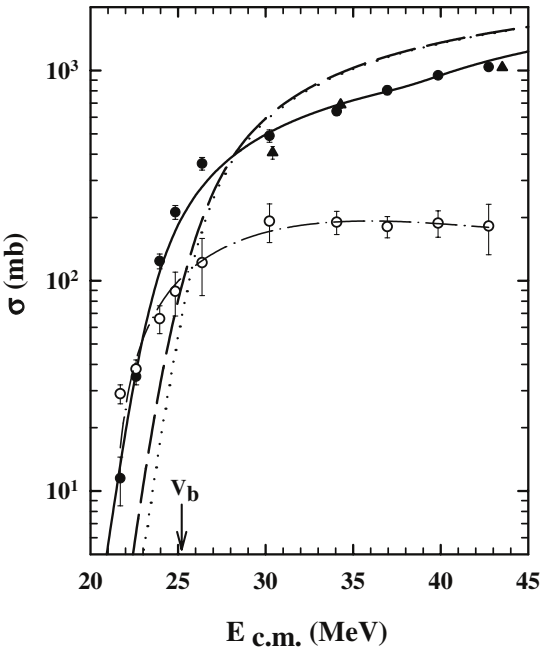

FIG. 1. Complete and partial breakup fusion cross section (filled and open circles) as a function of the center of mass energy for the ^{7}Li + ^{165}Ho system. The dotted curve is the prediction of a 1D-BPM calculation. The dashed and solid curves are the results of a coupled channel calculation including the effect of coupling to the ground state rotation band of the deformed target and only the breakup channel, respectively (see text). The solid triangles are the complete fusion cross sections for the ^{6}Li + ^{165}Ho system. The dash-dotted line is to guide the eye.

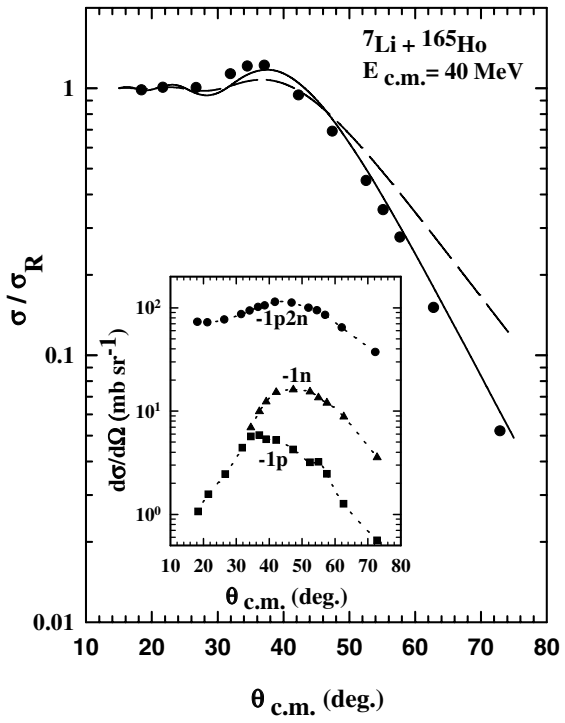

FIG. 2. Ratio of differential cross section for elastic(+ inelastic) to the Rutherford as a function of the scattering angle. The curves represent optical model calculations (see text). Shown in the inset are the Q-integrated differential cross sections for the $-1p$, $-1n$ and the inclusive α production (breakup) channels. The dotted lines are to guide the eye.

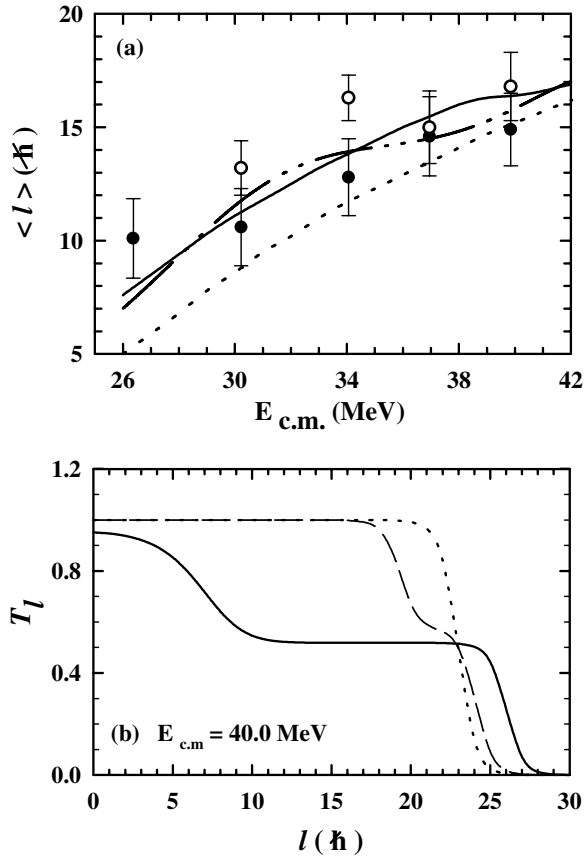

FIG. 3. (a) The average angular momentum as a function of the center of mass energy for the ^{7}Li + ^{165}Ho system. The solid and open circles are obtained from the measured γ-ray multiplicity and ratio of the evaporation residue cross section using a statistical model, respectively. The dash-dotted line is $\langle \ell \rangle$ obtained from a fit to the measured fusion excitation function. The solid curve is the predictions of coupled channel calculations including coupling to the breakup channel (the dotted curve is the 1D-BPM calculation). (b) Transmission coefficients, $T_\ell(E)$, as a function of ℓ at $E_{\text{c.m.}} = 40$ MeV corresponding to the curves in Fig. 1 (see text).

one nucleon transfer channels (40 and 12 mb for $-1n$ and $-1p$, respectively) highlight the importance of projectile breakup in the present system.

The average angular momentum, $\langle \ell \rangle$, for complete fusion was obtained using three methods, from the measured γ-ray multiplicity [21], ratio of the measured evaporation residues using a statistical model [22], and from a model independent analysis of the fusion excitation function [12,13]. An array of 14 hexagonal BGO detectors (63 mm $\times$ 57 mm) in a closed packed geometry, with a total efficiency of 66(0.02)% at 662 keV, was used in coincidence with the Compton suppressed HpGe detector for recording the fold distribution of the γ rays. The average multiplicity, $\langle M \rangle$, was obtained from the fold distribution for each channel by convoluting the response of the detector [23]. The $\langle M \rangle$ was converted into $\langle \ell \rangle$ taking into account the angular momentum carried per nonstatistical γ ray ($2\hbar$ for even A and $1.75\hbar$ for odd A), neutrons, and two statistical γ rays on an average each removing a mean angular momentum of $0.3\hbar$ and other corrections for each channel [21]. The average angular momentum of the compound nucleus was obtained by weighing the $\langle \ell \rangle$ for each channel by its partial cross section and is shown by the solid circles in Fig. 3(a). The errors in the $\langle \ell \rangle$ extracted arise mainly from the uncertainties in the conversion from $\langle M \rangle$ to $\langle \ell \rangle$ and are known to get worse for lower angular momentum due to the breakdown of the assumption of the stretched nature of the transitions. At a given excitation energy of the compound nucleus, the relative fractionation into different ER depends on the angular momentum distribution with which it is formed apart from factors such as density of the final state and barrier penetration [22]. The $\langle \ell \rangle$ was obtained using the statistical model code CASCADE by matching the calculated ratios $(3n/4n, 4n/5n)$ with the experimental ratios [open circles in Fig. 3(a)] using a consistent set of parameters which also reproduced partial cross sections in nearby systems. The errors arising only from the measured ratios are shown.

The $\langle \ell \rangle$ was also obtained from the measured fusion excitation function [dash-dotted line in Fig. 3(a)] [12–14]. As can be seen from Fig. 3(a) the measured values of $\langle \ell \rangle$ are consistent with those obtained from the fusion excitation function. The observed consistency implies that the assumptions discussed earlier regarding $T_l(E)$'s [12,13] are satisfied in the present problem, even in the presence of projectile breakup. This clearly indicates that any model used to explain the data must satisfy these assumptions.

The fusion cross sections and $\langle \ell \rangle$ calculated in a 1D-BPM model are shown in Figs. 1 and 3 (dotted curves), respectively, using the AW parametrization for the nuclear potential. It should be pointed out that the quantity of interest to be compared with model calculations is complete fusion and not complete + breakup fusion. At energies above the Coulomb barrier the CF cross sections are reduced by a factor of $\simeq 0.7$, compared to the predictions of the 1D-BPM and enhanced below it. The measured $\langle \ell \rangle$ are larger than the corresponding 1D-BPM predictions. These observations along with the consistency of the measured $\langle \ell \rangle$ with that obtained from the fusion excitation function validate the coherent nature of projectile breakup on fusion and thus the usage of a coupled channel approach. In the incoherent approach of breakup on fusion [5,6] the breakup survival probability contains a surface peaked imaginary potential leading to depletion of higher partial waves from the fusion process leading to a corresponding decrease in the $\langle \ell \rangle$ which is in contrast to the observations.

To illustrate the coherent effect of breakup on CF cross section and $\langle \ell \rangle$ in a coupled channel framework calculations using the code CCDEF [24] are presented. The role of target deformation in the present system was found to be small, despite the large value of $\beta_2 = 0.33$ for ^{165}Ho [14] (dashed curve in Fig. 1). Considering the dominance of breakup in the present case as compared to other channels, only two channels, elastic and breakup, were included

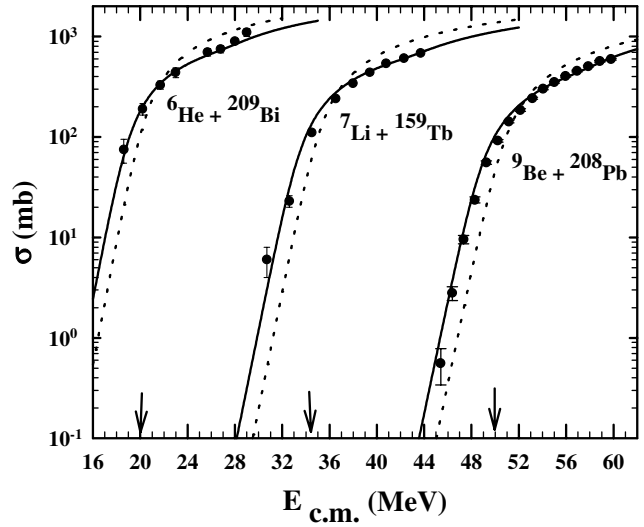

FIG. 4. The complete fusion cross sections for the ^{6}He + ^{209}Bi [10], ^{7}Li + ^{159}Tb [17], and ^{9}Be + ^{208}Pb [9] systems along with the coupled channel calculation (solid line) and 1D-BPM predictions (dotted line). The energy scales have been shifted for ^{7}Li + ^{159}Tb(+10 MeV) and ^{9}Be + ^{208}Pb(+11 MeV). The arrows indicate the Coulomb barriers for the corresponding systems.

in the calculation. The calculations were performed using a collective model inelastic form factor [20], $F(r)$, to simulate coupling to the breakup channel and are shown in Figs. 1 and 3 (solid lines). These calculations which required a large strength of the form factor, $F(r_B)$, are able to reproduce both the enhancement and reduction in the CF cross section and the increase in the $\langle \ell \rangle$, thus explaining the effect of projectile breakup on fusion. The increase in the $\langle \ell \rangle$ and decrease in cross sections at energies above the barrier due to coupling are illustrated in Fig. 3(b) where the transmission coefficients are plotted as a function of ℓ. The dotted, dashed, and solid curves are the calculations for the 1D-BPM, coupling to target deformation, and coupling to breakup, respectively, corresponding to the curves in Fig. 1. Calculations similar to that for the ^{7}Li + ^{165}Ho system using large values of $F(r_B)$, leading to two well separated barriers having nearly equal weights, for the ^{6}He + ^{209}Bi [10], ^{7}Li + ^{159}Tb [17], and ^{9}Be + ^{208}Pb [9] systems are shown in Fig. 4. These calculations reproduce both the enhancement below the barrier and reduction above for these systems. The coupled channel calculation by Hagino *et al.* [8] for the ^{11}Be + ^{208}Pb system also showed that a large strength is associated with coupling to the breakup channel in weakly bound nuclei, leading to an enhancement in cross section below and a reduction above the Coulomb barrier. Calculations with more realistic form factors for breakup, obtained using a cluster model for ^{7}Li, which are able to predict both the complete and breakup fusion, will further validate these conclusions [25].

In summary, the comparison of the measured complete fusion excitation function and average angular momentum with the 1D-BPM calculations showed an enhancement of cross section below the Coulomb barrier and decrease above it, along with an increase in $\langle \ell \rangle$. This conclusively points to the fact that breakup should be treated in a *coherent* manner like any other nonelastic channel. The above observations together with the consistency of the measured $\langle \ell \rangle$ with those obtained from the fusion excitation function justifies the use of the coupled channel approach for understanding the fusion of weakly bound nuclei. The results of the present work could have important implications on the use of RIB for the production of SHE, where energies around the barrier would be required to produce a relatively "cold" compound nucleus.

We thank C. V. K. Baba for many useful ideas and D. R. Chakrabarty, V. M. Datar, and S. Suryanarayan for fruitful discussions.

*Corresponding author.
Email address: navin@tifr.res.in

[1] B. M. Sherrill, Nucl. Phys. **A685**, 134c (2001).
[2] C. H. Dasso *et al.,* Nucl. Phys. **A405**, 381 (1983).
[3] M. Dasgupta *et al.,* Annu. Rev. Nucl. Part. Sci. **48**, 401 (1998); R. Vandenbosch, *ibid.* **42**, 447 (1992).
[4] C. Signorini, Nucl. Phys. **A616**, 262c (1997).
[5] M. S. Hussein *et al.,* Phys. Rev. C **46**, 377 (1992).
[6] N. Takigawa *et al.,* Phys. Rev. C **47**, R2470 (1993).
[7] C. H. Dasso *et al.,* Phys. Rev. C **50**, R12 (1994).
[8] K. Hagino *et al.,* Phys. Rev. C **61**, 037602 (2000).
[9] M. Dasgupta *et al.,* Phys. Rev. Lett. **82**, 1395 (1999).
[10] J. J. Kolata *et al.,* Phys. Rev. Lett. **81**, 4580 (1998); P. A. DeYoung *et al.,* Phys. Rev. C **62**, 047601 (2000).
[11] M. Trotta *et al.,* Phys. Rev. Lett. **84**, 2342 (2000).
[12] C. V. K. Baba, Nucl. Phys. **A553**, 672c (1993).
[13] A. B. Balantekin *et al.,* Phys. Rev. C **33**, 379 (1986); A. B. Balantkin, in *Proceedings of the JAERI International Symposium,* edited by Y. Sugiyama (Universal Academy Press, Tokyo, 1988).
[14] A. Navin *et al.,* Phys. Rev. C **54**, 767 (1996).
[15] F. Pulhofer, Nucl. Phys. **A280**, 267 (1975); D. R. Chakrabarty (private communication).
[16] A. V. Ignatyuk *et al.,* Sov. J. Phys. **21**, 255 (1975).
[17] R. Broda *et al.,* Nucl. Phys. **A248**, 356 (1975).
[18] H. Utsunomiya *et al.,* Phys. Rev. C **28**, 1975 (1983).
[19] J. Raynal, Phys. Rev. C **23**, 2571 (1981).
[20] R. A. Broglia and A. Winther, *Heavy Ion Reactions* (Addison-Wesley Publishing Company, Redwood City, CA, 1991), Vol. 1.
[21] A. H. Wuosmaa *et al.,* Phys. Lett. B **263**, 23 (1991); R. D. Fischer *et al.,* Phys. Lett. B **171**, 33 (1986).
[22] M. Dasgupta *et al.,* Phys. Rev. Lett. **66**, 1414 (1991).
[23] S. Van der Werf, Nucl. Instrum. Methods **153**, 221 (1978).
[24] J. Férnandez-Nielo *et al.,* Comput. Phys. Commun. **54**, 409 (1989).
[25] A. Vitturi (private communication).